PAPER Nr.: 53

# Active Expansion of Helicopter Flight Envelope

Marcel KRETZ
Chief Engineer

GIRAVIONS DORAND Industries

92150 SURESNES, FRANCE

**FIFTEENTH EUROPEAN ROTORCRAFT FORUM**

SEPTEMBER 12 - 15, 1989 AMSTERDAM

# ACTIVE EXPANSION OF HELICOPTER FLIGHT ENVELOPE

Marcel KRETZ
Chief Engineer

GIRAVIONS DORAND Industries, 92150 SURESNES, FRANCE

Abstract

In search for high load factors, necessary in air-to-air and NOE combat missions, and for speed to increase the general helicopter performance, the use of active controls is proposed. More particularly, the stall barrier feedbacks are found well adapted to bring higher lift capability and much more efficient, vibration-free rotor working conditions.

The paper relates recent research effort done under French Government, DRET Research Agency, contracts to develop active controls to enlarge the helicopter flight envelope well beyond the present stall barrier limit.

The new findings concern the rotor lift capability and the existence of rotor instability in the $\bar{C}_L$ region above the rotor stall barrier. In fact, for higher lift values, then those demonstrated in the wind tunnels, the rotor has to be stabilized either by the human pilot or artificially, by active means.

The origin of the high $\bar{C}_L$ instability can be traced down to the saturation of the retreating blade, to the cancellation of blade damping, and to the azimuthal velocity variations. The stability limit can be determined experimentally by analysing the behaviour of the control matrix, which becomes singular at the stability limit. To remedy these difficulties a new mode of rotor control is proposed.

It is based essentially on a specific lift variation acting over the rotor region of the advancing blade and over the fore-and-aft disk sectors.
Active control technology is employed to process the detection signals coming from local pressure pick-ups and blade flapping sensors, to stabilize the rotor and optimize the control laws.
The direct result of these actions are power gains. In a typical example, gains of 17,3 % of rotor power are attained at $\bar{C}_L = 0{,}75$ and $\mu = 0{,}3$. The paper concludes with applications of the stall barrier feedbacks to expand the helicopter flight envelope.

## 1. Introduction

In this paper we present the main results of a several years research work oriented towards the expansion of helicopter flight envelope. The study has been done under French Government, DRET Research Agency, contracts and covers the development of active means to shift the present stall barrier limits.
The earlier work in this field, refs. 1 and 2, has shown that the stall barrier feedbacks envisaged can bring considerable power gains. Subsequently, we discovered the nature of the rotor limitations appearing at high lift coefficients, $\bar{C}_L$ , and proposed the introduction of artificial stability to avoid the stall effects and modify the basic dynamic responses of the rotor, ref. 3, above the stall barrier.

## 2. Main definitions

$\bar{C}_L$ = 6 $C_T/6$, mean lift coefficient as defined in ref. 4, page 287.
$\bar{S}_f$ = $f/A6$ reduced frontal area drag coefficient.
$\beta$ = a0 ($\Psi$) − a1 ($\Psi$) cos$\Psi$ − b1 ($\Psi$) sin$\Psi$ , this formula defines the variable conicity a0 ($\Psi$) and the disk position: a1 ($\Psi$) and b1 ($\Psi$).
a1 ($\Psi$) gives the instantaneous longitudinal rotor tilt, derived from the flapping angle of a single blade, $\beta$.
b1 ($\Psi$) gives the lateral instantaneous disk position.
SB Stall Barrier The SB is defined experimentally, in a wind tunnel, as the maximum lift limit derived from $\bar{C}_L$ ($\theta_0$) curves for a fixed reduced frontal area drag coefficient, $\bar{S}_f$.
Theoretically, the stall barrier is defined by the singularity conditions of the control matrix. It can be shown that the two definitions of the SB coïncide.
CM Control Matrix The CM links the lift and longitudinal disk variations with the main control inputs: $\theta_0$, collective pitch, and $\theta_{1s}$ cyclic longitudinal pitch.

$$\begin{bmatrix} \Delta\ \bar{C}_L/a \\ \Delta\ a_1 \end{bmatrix} = \begin{bmatrix} \\ CM \\ \\ \end{bmatrix} \begin{bmatrix} \Delta\theta_0 \\ \Delta\theta_{1S} \end{bmatrix}$$

## 3. Stall Barrier, SB

We will, first of all, concentrate on the physical aspects of the stall barrier.
Fig. 1, ref. 5, shows typical wind tunnel and flight envelopes. On examining closer these results, we remark that the flight boundaries are located well above the wind tunnel limits. We find a similar situation in figure 2, ref. 2 and ref. 6. It follows that somehow the rotor is capable to produce much more lift in flight that in the wind tunnel. The dynamic aspects of the pitching velocity, analysed in ref. 7, do not explain the considerable lift increase shown in flight tests. As we can see, the highest value attains a mean lift coefficient of 1.2. The literature seems particularly silent about the rotor working conditions above the stall barrier. We know from flight tests that the helicopter shows a strong tendancy to pitch up at high load factors, with a possible control loss, when the load factors exceed some limit values. The deterioration of the flying qualities is notorious in this case. In ref. 8, an operational limit of the helicopter envelope is presented, fig. 3. This limit is based on the value of the partial derivative of the mean lift coefficient with respect to the collective pitch. A 33 % reduction of this derivative corresponds to a flying qualities boundary "beyond which the pilot experiences a significantly degraded response to control input".

To analyse more closely this aspect, we defined the control matrix, CM, see "Main Definitions". This matrix when multiplied by the control inputs, the collective and cyclic pitch, gives the lift and the rotor tilt variations. The CM contains four elements, one of them corresponds to the partial derivative used in ref. 8. Fig. 4 shows an analytical result based on the E52 rotor used in our earlier wind tunnel tests, ref. 1. We have traced here the four derivatives against the mean lift coefficient $\bar{C}_L$ . We remark a comparatively slow variation of their value with $\bar{C}_L$. However, when we look at the determinant of the matrix, we see its' rapid decrease leading to zero at the singular value of $\bar{C}_{L_{sing.}} = 0{,}68\ \bar{C}_{L_{max.}}$ Curiously, for this $\bar{C}_L$ value, the BOEING derivative attains its critical 67 % level. At this point the CM becomes singular. In practice, for the corresponding $\bar{C}_L$ levels the computer models, based on iterative procedures, become divergent and no solutions can be obtained. A similar result has been encountered using the characteristics of a particular Aerospatiale test rotor 7A, ref. 9, experimented in the ONERA 8 m diam. S1MA wind tunnel, fig. 5.

We remark that in the vicinity of the singular value of $\bar{C}_L$, the computer code fails to converge to a solution. Erratic results have been obtained in this case. We can estimate the $\bar{C}_{L\,sing}$ only by extrapolation of the curve showing the variation of the CM determinant tending to zero. Parallel to this analysis, when we determine the lift limit for the same reduced drag area $\bar{S}_f$, we find that the maximum of the $\bar{C}_L$ $(\theta_o)$ curve corresponds to the singular value of $\bar{C}_L$. This can be demonstrated analytically: the variations of the lift and propulsion (or rotor forward tilt) being zero, the CM becomes singular by the fact that the basic equations have no solution.

The conclusion of this study is significant. It shows that the present control system looses, at that singular point, its effectiveness and becomes no more capable to ensure further increase of the rotor lift. We are, in this case, at the accessibility limit of the wind tunnel tests.
Our first conclusion, as we can see in fig. 1, is apparantly in contradiction with flight tests which show that much higher $\bar{C}_L$ can be obtained than in wind tunnels and that a conventional rotor can work above the stall barrier in conditions which we will try now to clarify.

## 4. Rotor behaviour above the Stall Barrier

We have started our presentation with the analysis of the rotor behaviour below the SB, a field of investigation that is experimentally accessible in the wind tunnels and is well known except in the vicinity of the SB. Uncertainties of rotor aerodynamics and comparative lack of flight results at high load factors make the following analysis more hypothetical and we have to rely on the rare test results and extrapolations of the theoretical rotor models, validated up to the SB. Nevertheless, the results of our study seem to be well established and correlate correctly with the present experience of rotors working at high $\bar{C}_L$ values.
Our first attempts to penetrate the SB were fruitless. We remarked, however, that in the $\bar{C}_L - \mu$ domain, above the SB, one of the itineration conditions, nulling the aerodynamic blade flapping moment $\bar{M}_{1s}$ (proportional to $+ \sin\psi$), is particularly difficult to render zero. This phenomenon soon showed to be the main origin of rotor divergence. In fact, the $\bar{M}_{1s}$ moment is responsable of the rotor pitch-up at high load factors. The physical aspects of this instability can be traced

down to the saturation of the rotor in a particular, ideal, case when the entire rotor works at a constant $C_{l}$. The flapping equation becomes:

$$\ddot{\beta} + \beta = \frac{C_{l0}}{2a}\gamma\int_0^1 v^2 r\,dr = \frac{C_{l0}}{8a}\gamma\left(1 + \frac{8}{3}\mu\sin\psi + 2\mu^2\sin^2\psi\right)$$

the $+\sin\psi$ term

We remark that the aerodynamic forcing moment, present on the left side of the flapping equation, contains a $+\sin\psi$ term that causes a divergent blade motion, as shown in fig. 6. The origin of the rotor instability stems from a combined action of blade saturation due to stall and velocity variations due to the forward speed of the helicopter. We remark that the aerodynamic damping vanishes at the same time.
The blade is in state of resonance, excited by a one-per-rev aerodynamic moment: $\frac{C_{l0}}{3a}$

$$\overline{M}_{1S}\sin\psi = A\sin\psi \qquad A = \mu\frac{C_{l0}}{3a}\gamma$$

having the following solution, and showing the characteristic pitch-up of the rotor:

$$\beta = -\frac{1}{2}A\psi\cos\psi$$

$$a_1(\psi) = \psi\frac{A}{2} \qquad b_1(\psi) = 0$$

This particular instability is comparatively favourable when compared with the exponental divergence of many other unstable systems and can be, as the facts show, mastered by the human pilot. However, it can not be reproduced in the wind tunnel by conventional means. Thus we come to the second conclusion that the rotor is unstable when operating above the SB and that the presence of the human pilot is necessary to stabilize the aircraft in this case.
Having illustrated the mechanism of the rotor instability, when working above the SB, we will present now means capable to render the rotor stable.

## 5. New mode of rotor control

The two conclusions drawn from the study of the SB indicate that the expansion of the rotor operating domain beyond the SB needs not only the introduction of a stabilization means of the rotor, but that, first of all, we have to create a new control mode. In fact, the study has shown that the conventional control mode becomes inefficient in the neighbourhood of the SB.

In consequence, the appearance of stall on the retreating blade has a double ill-action. It generates instability and renders the present controls inactive. The retreating blade being aerodynamically ineffective, in search of a solution we turned our attention towards the advancing blade, who works under sound aerodynamic conditions. The analysis of lift variations in the 0 ° to 180 ° azimuth sector gave rise to a new mode of rotor control, ref. 3. Ideally, we can imagine a flapping moment acting in this sector that makes the rotor disk tilt forward to compensate for the pitch-up generated by the stall. Such a moment has, at the same time, to have a lift distribution giving no resultant lift variation on the disk. Fig. 7 illustrates the specific law of lift variation satisfying these conditions. There are three local variations centered round the azimuth angles 0 °, 90 °, 180 °. The shape of the lift impulses is the same and corresponds to:

| | | |
|---|---|---|
| ½ cos $3\Psi$ | in sector | −30 ° to +30 ° |
| sin $3\Psi$ | in sector | +60 ° to +120 ° |
| −½ cos $3\Psi$ | in sector | +150 ° to +210 ° |

On the advancing blade, the amplitude of the impulse is doubled. From fig. 7 it is evident that the specific law presented, creates a $-\sin\Psi$ flapping moment that can balance the destabilizing moment stemming from the stall action on the retreating blade. At the same time the resultant force distribution is zero. It should be stressed here, that we impose on the blade a lift variation and not a pitch variation. This necessitates the detection of local pressures on the blade. In particular, the pressure near the leading edge, ref. 1, is representative of the local lift value.

The introduction of the specific law variation of the lift permits, by creating a $\sin\Psi$ flapping moment, to tilt the rotor in the plane at 90 °, in the same manner as does the conventional swash-plate inclination. However, the β damping effect is lacking in our case and we have to replace it by a second loop based on the detection of the blade flapping angle β referenced by a plane controlled by the pilot. This later effect replaces the swash-plate action. Fig. 8 gives a simplified block diagram of the new control system. The system has three inputs $\theta_{1c}$, $\theta_{1s}$ and $\theta_0$, that replace the conventional cyclic and collective pitch. Their role is to serve as references in the feedback loops.

The comparison of inputs and outputs generates the following error signals:

| | | |
|---|---|---|
| $\epsilon = \theta_{1s} - a_1$ | $\epsilon = \theta_{1c} - b_1$ | $\epsilon = \theta_0 - C_\ell$ |
| Longitudinal control | Lateral control | Lift control |

The signals $a_1$ , $b_1$ , $C_\ell$ are mesured outputs. The longitudinal and lateral control errors are affected by their respective specific laws and added to the lift control error before acting on the blade pitch actuator, supposed to be located on the rotating part of the rotor hub.
The actuator, for simplicity represented as a pure integrator, constitutes together with the blade generating the lift $C_\ell$ (obtained from local pressure measurements) the inner feedback loop, shown in heavy lines in fig. 8.

There are two outer loops corresponding to the longitudinal $a_1(\Psi)$ and lateral $b_1(\Psi)$ output signals. These are determined by an identification procedure from the mesured flapping angle $\beta$. We have to mention that the rotor position is a non-mesurable parameter and has to be deduced from the flapping angle $\beta$ by an arbitrary relationship. To express the rotor tilt we have chosen for simplicity:

$$\beta(\Psi) = a_0(\Psi) - a_1(\Psi)\cos\Psi - b_1(\Psi)\sin\Psi$$

Where $\beta(\Psi)$ can be any time varying function.
The new mode of rotor control, presented in fig. 8, though principally proposed to solve the rotor instability problem above the SB, can operate in all rotor configurations, in forward speed and at hower, as well as at higher load factors configurations.Using the stall barrier feedback of fig. 8 we studied the dynamic behaviour of the rotor at high $\bar{C}_L$ values, where the instability appears. The highest value attained was 1.1. Figures 9 and 10 illustrate the rotor responses corresponding to four different values of mean lift coefficient $\bar{C}_L$. The input is a step fonction equivalent to a backward stick inclination. In fig. 9 we are at the edge of the SB. A step of 3 ° has been applied during 12 revolutions. The rotor attains here its position roughly at the end of the first rev. The transient dies out to show a perfectly stable rotor position.

Studies are under way to reduce vibrations and coupling effects. The lateral coupling amplitude is of the order of 50 % of the main rotor tilt and is damped out after three revolutions. Fig. 10 shows similar responses at higher $\bar{C}_L$ values: 0.9, 1.0, 1.1. With the characteristics of the SB feedback unchanged, there exists a general tendancy of deterioration of the transient responses. Also, the coupling effects become more important and become slower to be damped.
Of course, these results, obtained comparatively recently, show a wide area of investigation for future applications, .

## 6. Power gains

Before concluding this paper, we would like to recall that the original purpose of SBF (Stall Barrier Feedbacks), as presented in ref. 1, were the power gains. This objective, of course, still holds good. In the domain below the SB, these gains are obtained by elimination of stall conditions. This is done by introduction on the retreating blade of adequate pitch variation laws to maintain the aerodynamic working conditions under the stall point. Wind tunnel results obtained with simplified SBF s gave already an encouraging gain of 8 % with an advance ratio of 0,3 and a mean lift coefficient of 0,6, ref. 2. Much higher power gains are obtained when we approach the SB.

We present in figure 11 an analytical result obtained using the 7A rotor. At $\bar{C}_L = 0{,}75$ and $\mu = 0{,}3$, the power gain attains 17,3 % in a suboptimal case. The optimisation was done on eight parameters to determine the corresponding pitch variation, fig. 12.

As shown in fig. 11 the power gain is essentially obtained on the retreating side of the rotor disk by avoiding the drag divergence due to stall. This condition is approached simultanously by two different control actions on the rotor. On the retreating side, the angle of attack is reduced by a combined action of the conventional control and the additional pitch law of fig. 12. On the advancing side, the control action tilts the rotor forward by reducing locally the pitch angle. It must be remarked that the forward tilt of the rotor disk is particularly favourable in stall avoidance techniques.

Above the stall barrier, no wind tunnel power measurements are possible and the test results are uncertain. Therefore the power gains can not be estimated at very high $\bar{C}_L$ values. However, analytical results using SB feedback stabilizing the rotor can be obtained. Recent computations, carried out in suboptimal conditions, are shown in fig. 13. The heavy line indicates the power absorbtion coefficient $\bar{C}_P = 8\, C_P/\sigma$ for lift variations attaining $\bar{C}_L = 1.1$. From the figure it seems evident that we can expect considerable power gains at very high $\bar{C}_L$ values associated with much higher level of flying qualities.

## 7. Conclusions

In conclusion we have listed below the main results of our study concerning the rotor behaviour above the stall barrier:

1. The stall barrier denotes a limit of stable rotor behaviour.
2. The stall barrier coincides with lift limit of wind tunnel tests.
3. With increase of lift beyond the stall barrier:

Firstly: The conventional blade control becomes ineffective.
Secondly: The damping capacity of the blade vanishes.
Thirdly: The rotor becomes divergent.

4. The loss of rotor control in the vicinity of the stall barrier can be mesured by observing the change of the control matrix characteristics.
5. The lack of the blade damping leads to a typical rotor pitch-up stemming from the incapability of the blade to counter the $+ \sin\Psi$ flapping moment excitation.
6. The one-per-rev. blade excitation, that gives rise to the rotor pitch-up, originates from the azimuthal velocity variations and thus has the $+ \sin\Psi$ dynamic characteristics.
7. Predetermined passive control laws, compensating the $+ \sin\Psi$ excitation, do not permit to control the rotor position.
8. The stall barrier feedback represents a solution that eliminates the three phenomena (see above point 3) that trouble the rotor behaviour when it is operating above the SB.

## 8. Final Remarks

The final remarks are separated from conclusions, as they contain certain unverified assumptions that can, however, be reasonably formulated from the present results:

1. The active control has the potential of widening considerably the helicopter flight envelope. This can be achieved by shifting the stall barrier towards higher $\bar{C}_L$ and higher $\mu$. In forward flight, at $\mu = 0,3$, $\bar{C}_L$ of 1.2 are feasable in artificially stabilized conditions.

2. The limitations due to stall effects can be overcome by stall barrier feedbacks avoiding stall conditions and stabilizing artificially the rotor dynamic behaviour.

3. High order optimization of control inputs is essential to obtain power gains, higher speeds, satisfactory flying qualities and elimination of vibrations.

4. The solutions proposed are based on sensing the local aerodynamic pressures and the flapping angles on the blades.

5. At high load factors the stall barrier feedback supplements or replaces the conventional control by a new system acting on the advancing side of the rotor disk as well as on the retreating side.

6. A generalized application of the active control technology would lead to redefinition and readaptation of the helicopter rotor, the optimal L/D ratio being shifted towards higher $\bar{C}_L$ levels.

7. Additionally, the stall barrier feedback increases the safety margins in power loss event and during autorotational landings.

8. The stall flutter is entirely eliminated.

The general remark that can be made for the future is that in search for high load factors, necessary in air-to-air and NOE combat missions, and for high speed to increase the general helicopter performance, the use of active controls is necessary. More particularly, the stall barrier feedbacks are found well adapted to bring higher lift capability and much more efficient, vibration-free rotor working conditions.

## 9. References


1. Kretz M. : "Active Elimination of Stall Conditions" 37th Forum of the American Helicopter Society, May 1981.
2. Kretz M. : "The Impact of Active Control on Helicopter Handling Qualities" AGARD Conf. Proc. N° 333, March 1982
3. Kretz M. : "Procédé et dispositif de commande d'une voilure tournante" French Patent N° 2 607 465, 1st December 1986
4. Johnson W. : "Helicopter Theory", Princeton University Press, 1980
5. Philippe J.J. and Vuillet A. "Aerodynamic Design of Advanced Rotors with new tip shapes" 39th Forum of the AHS, May 1981
6. Van Gaasbeek J.R. : "An Investigation of High - G Manoeuvres of the AH-1G Helicopter" USAAMRDL-TR-75-18, April 1975
7. Brown E.L. and Schmidt P.S. : "The effect of helicopter pitching velocity on rotor lift capability" J. American Helicopter Society, October 1963
8. Mc. Veigh M.A. and Mc. Hugh F.J. "Recent Advances in rotor technology at Boeing Vertol" 38th Forum of the AHS, May 1982
9. Drevet J.P. and Guillet F. "Essais comparés de rotors d'hélicoptère en soufflerie" ONERA TP N° 1982-119, November 1982

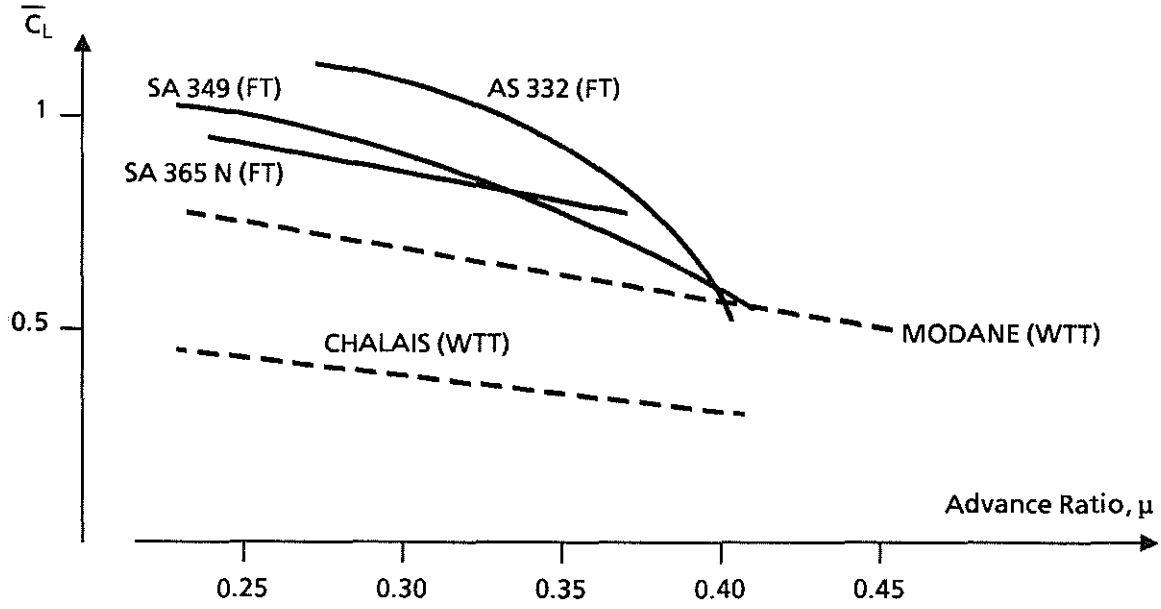


**Fig. 1 : AEROSPATIALE ROTORS : WIND TUNNEL AND FLIGHT TEST ENVELOPES (Ref. 5)**

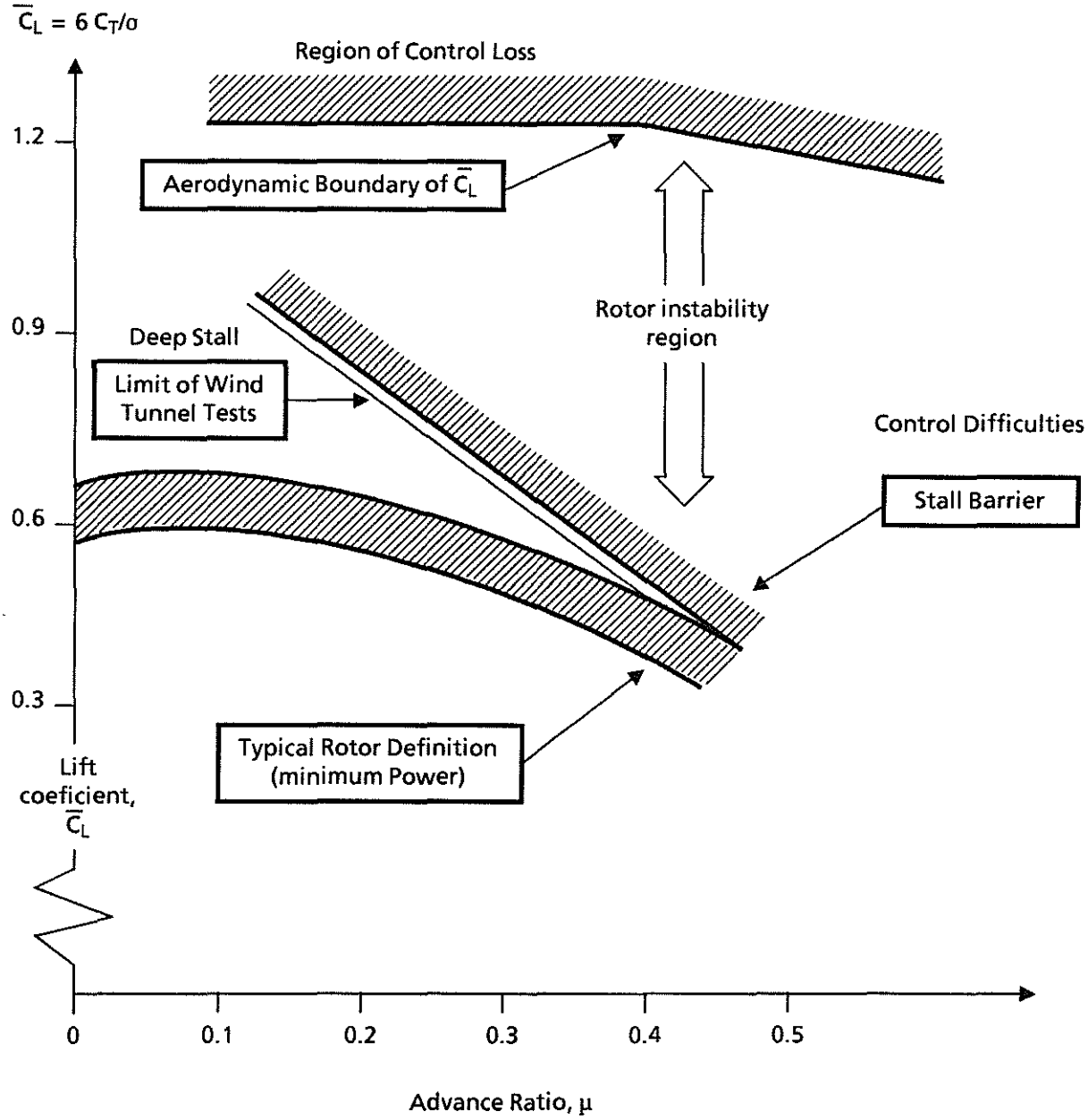


**Fig. 2 : Flight envelope**

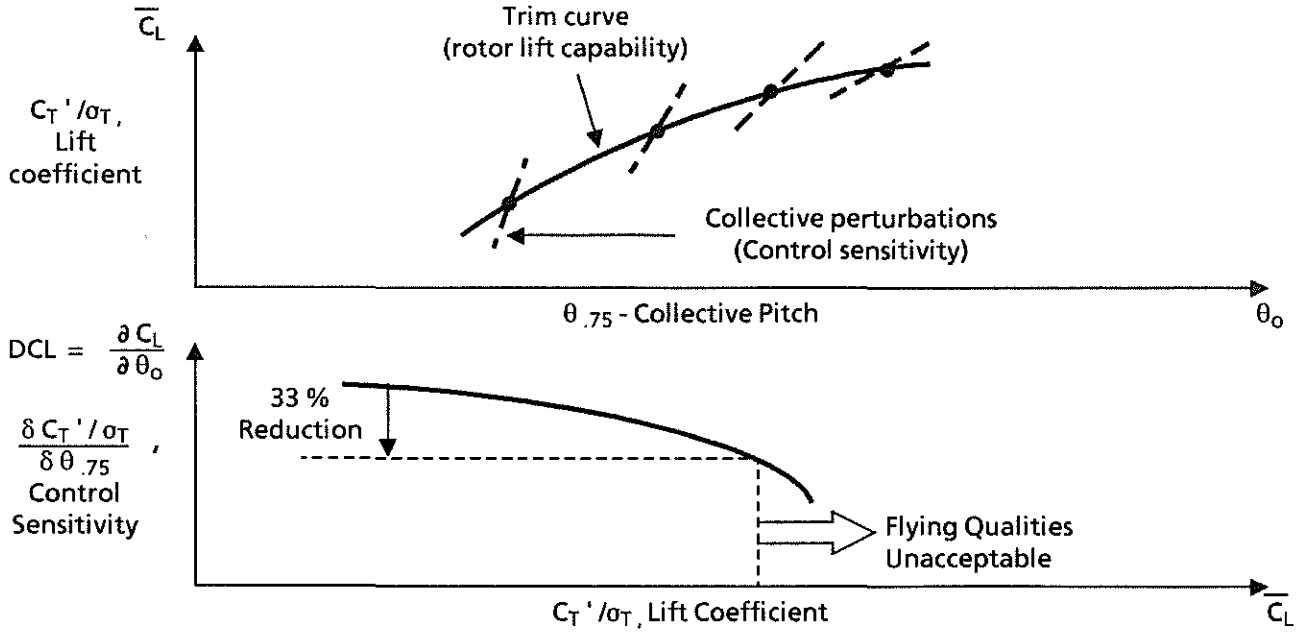


**Fig. 3 : DEFINITION OF FLYING QUALITIES LIMIT (Ref. 8)**

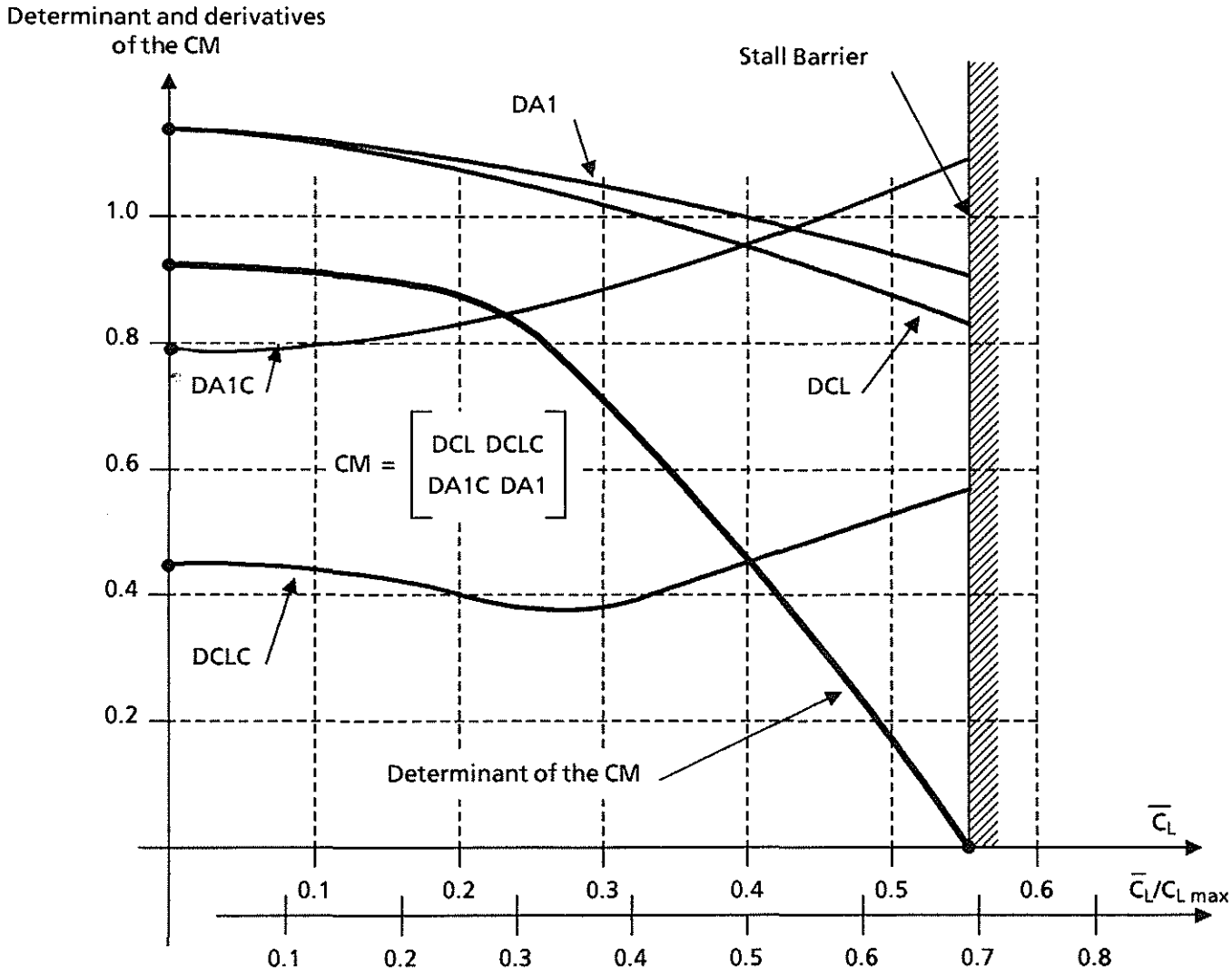


**Fig. 4 : DEFINITION OF THE STALL BARRIER (E52 ROTOR)**

**$\mu$ = 0.3 $\overline{S_f}$ = 0.15**

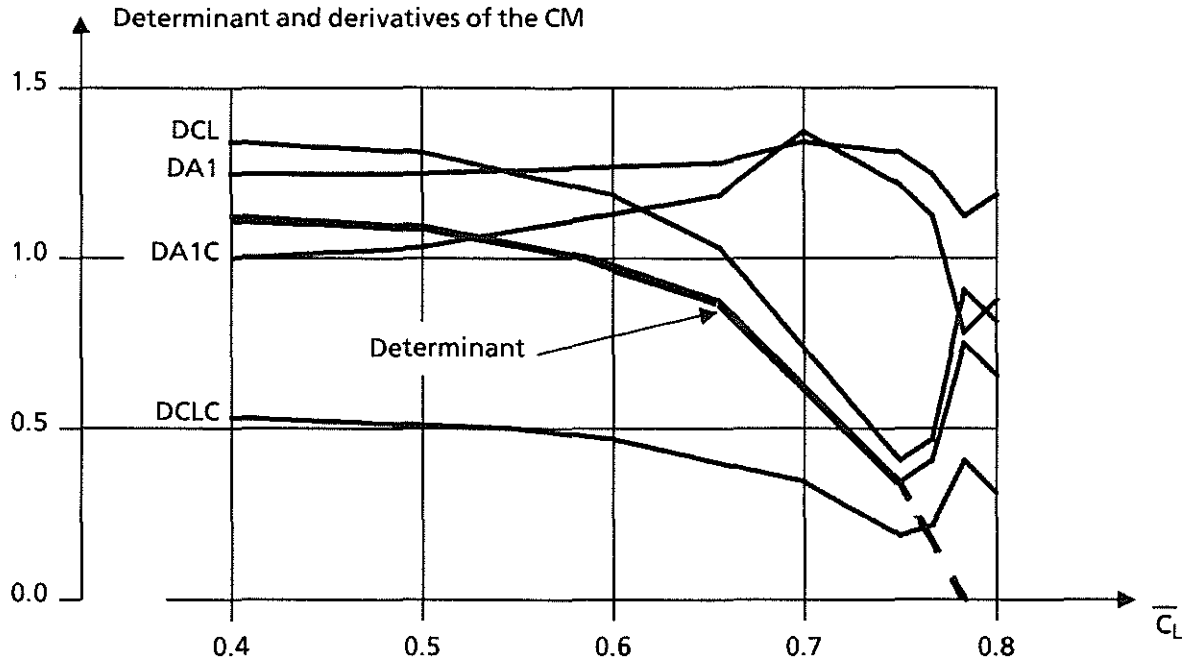


**Fig. 5 : DEFINITION OF THE STALL BARRIER (7A ROTOR)**

$\mu = 0.3 \quad \overline{S_f} = 0.10$

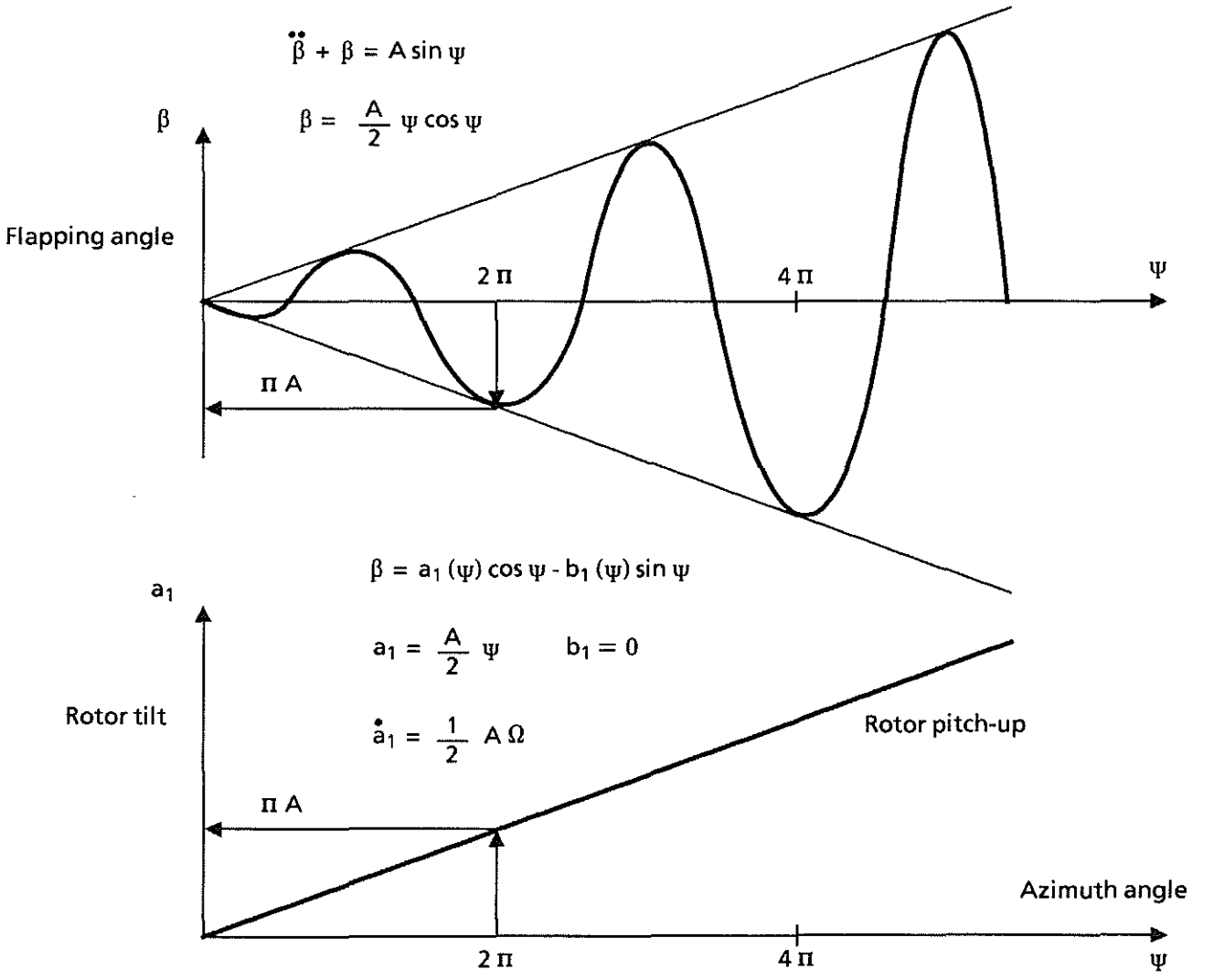


**Fig. 6 : BLADE DIVERGENCE**

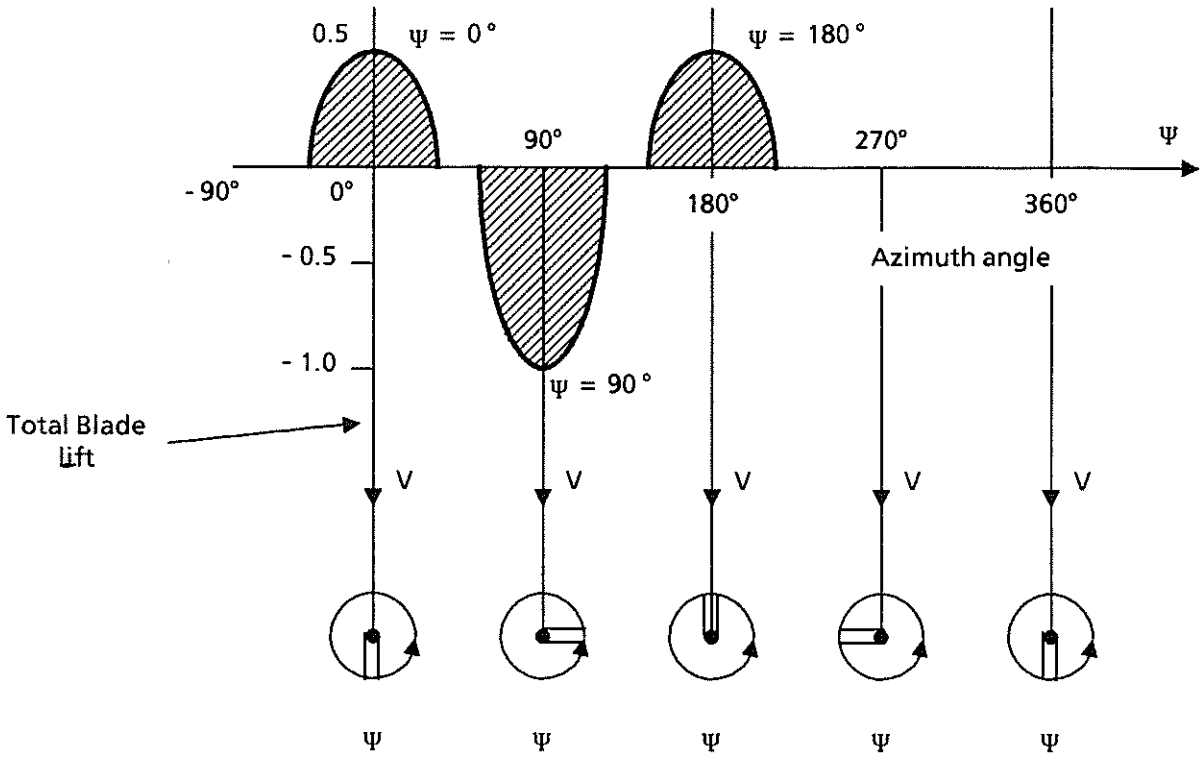


**Fig. 7 : SPECIFIC LAW OF LIFT VARIATION (Ref. 3)**

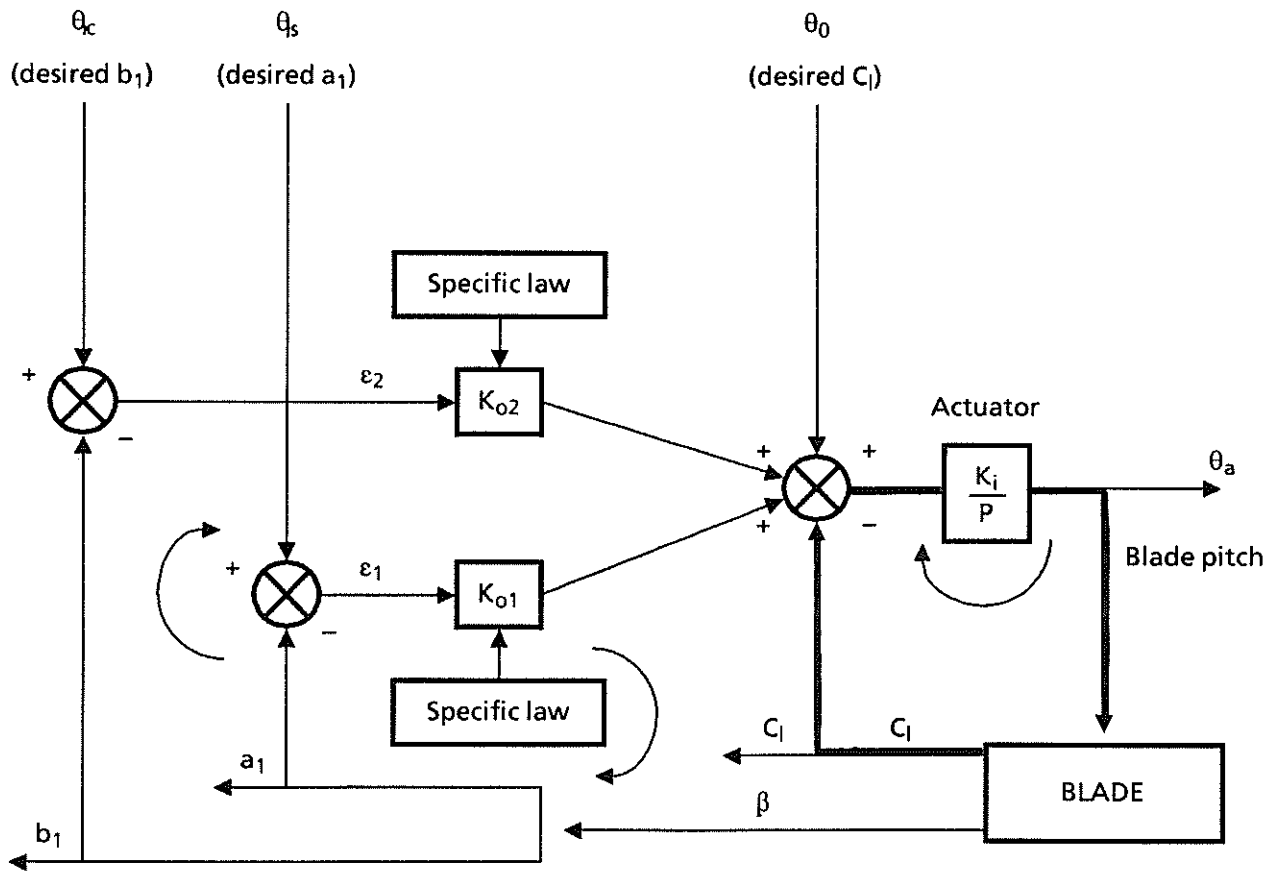


$$\beta(\psi) = a_0(\psi) - a_1(\psi)\cos\psi - b_1(\psi)\sin\psi$$

**Fig. 8 : SIMPLIFIED DIAGRAM OF THE NEW CONTROL SYSTEM (Ref. 3)**

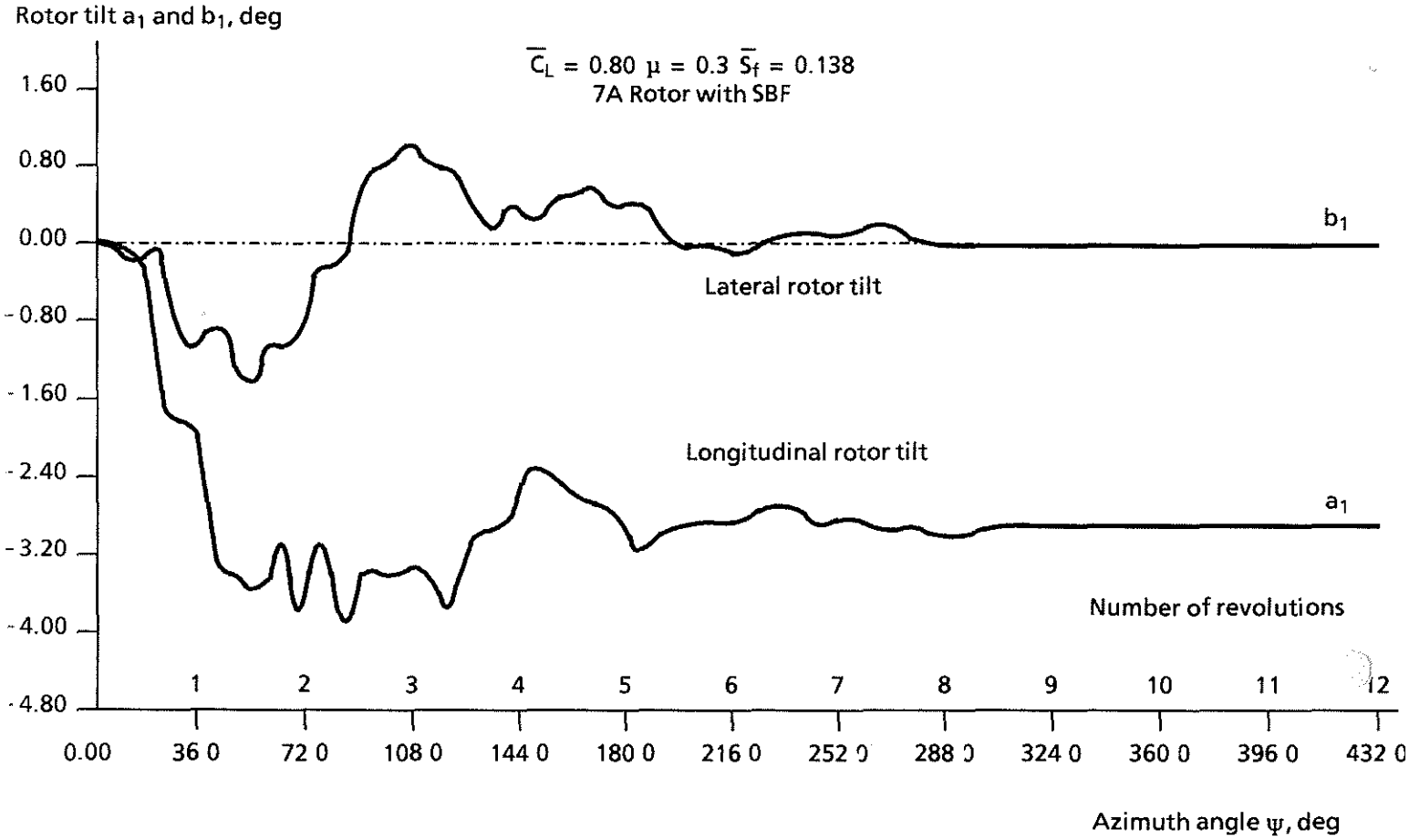


**Fig. 9 : ROTOR RESPONSE TO A STEP INPUT AT STALL BARRIER**

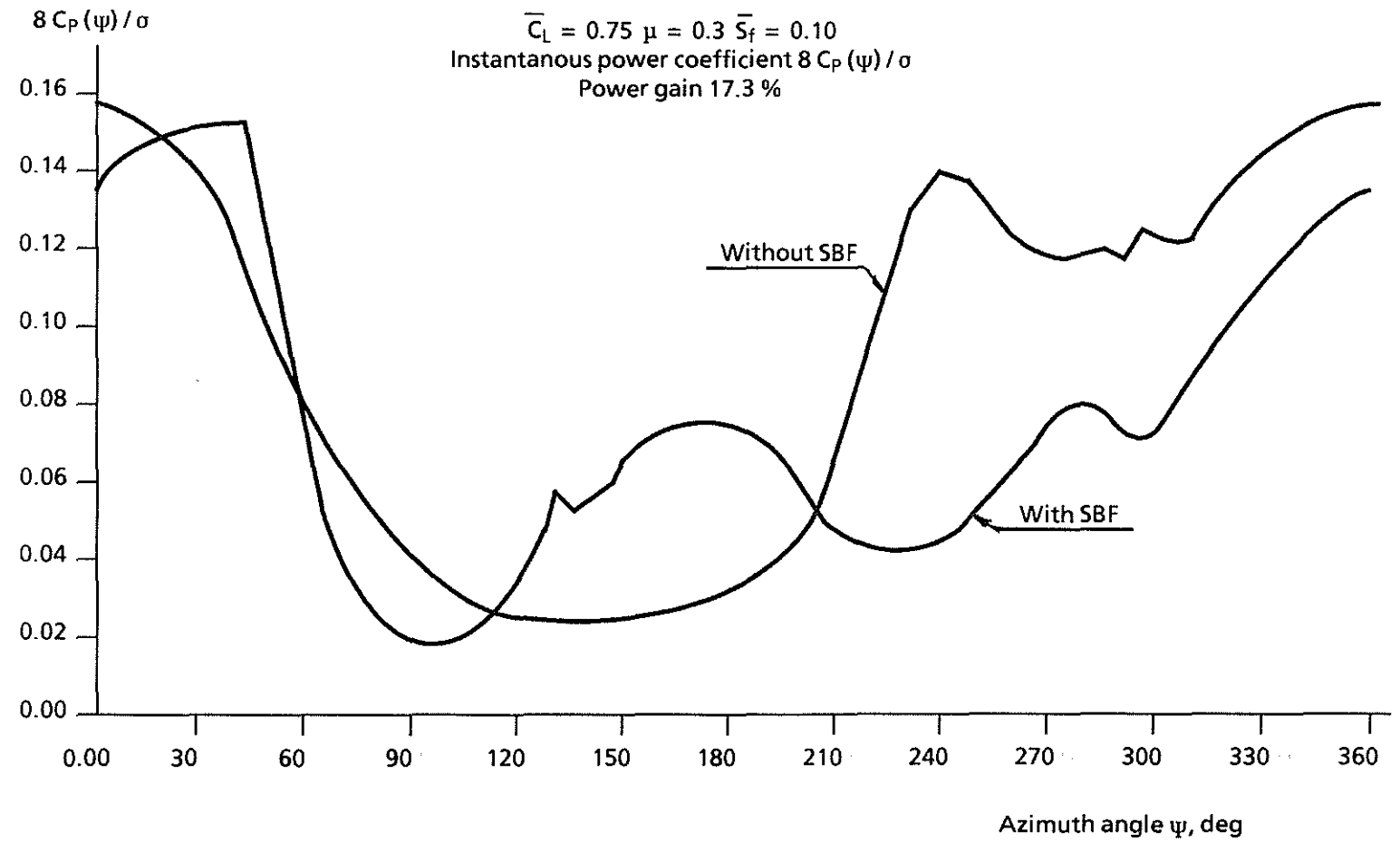


**Fig. 11 : COMPARISON OF INSTANTANOUS POWER COEFFICIENTS WITH AND WITHOUT STALL BARRIER FEEDBACK**

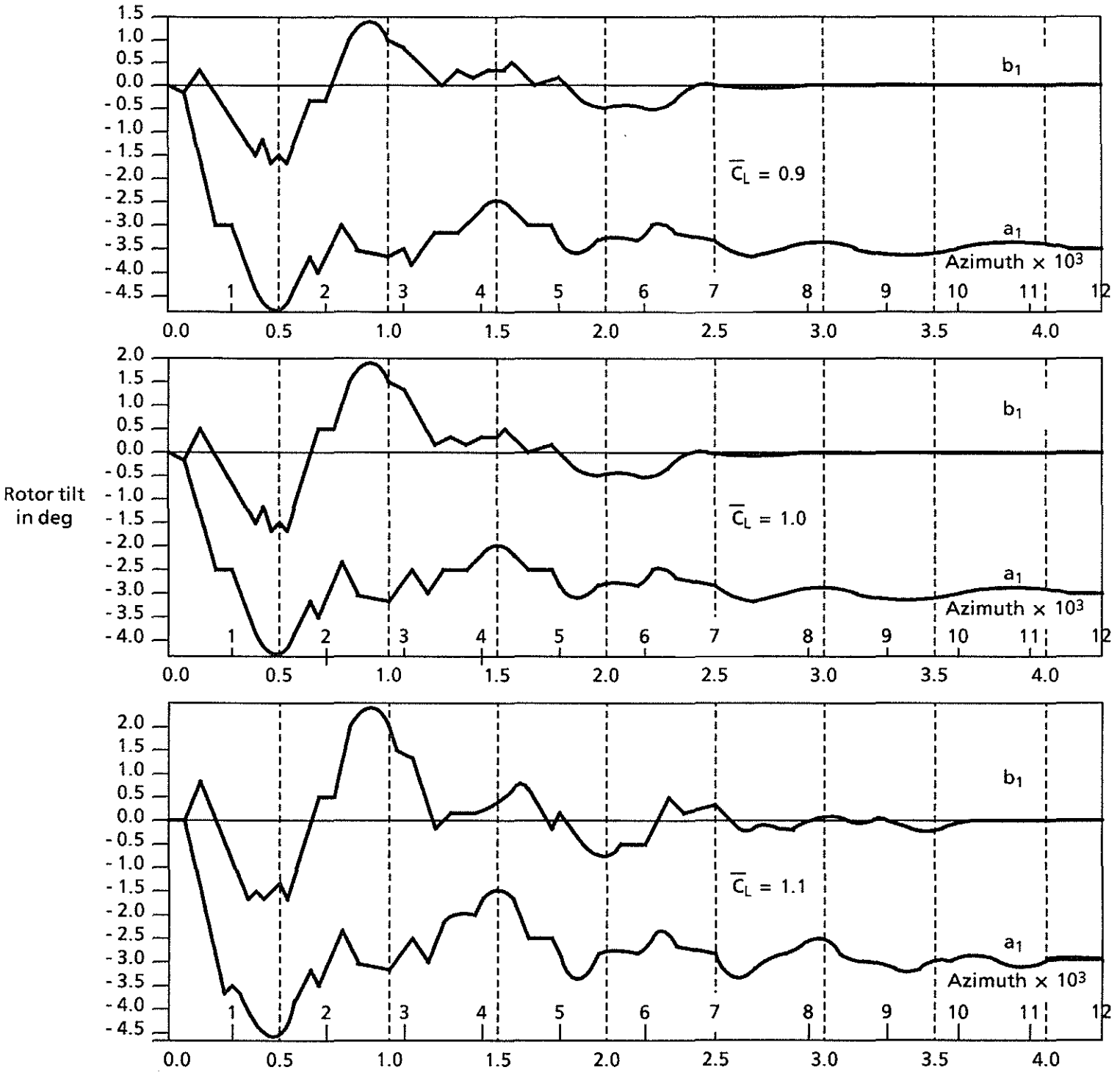


**Fig. 10 : ROTOR RESPONSES TO A STEP INPUT**

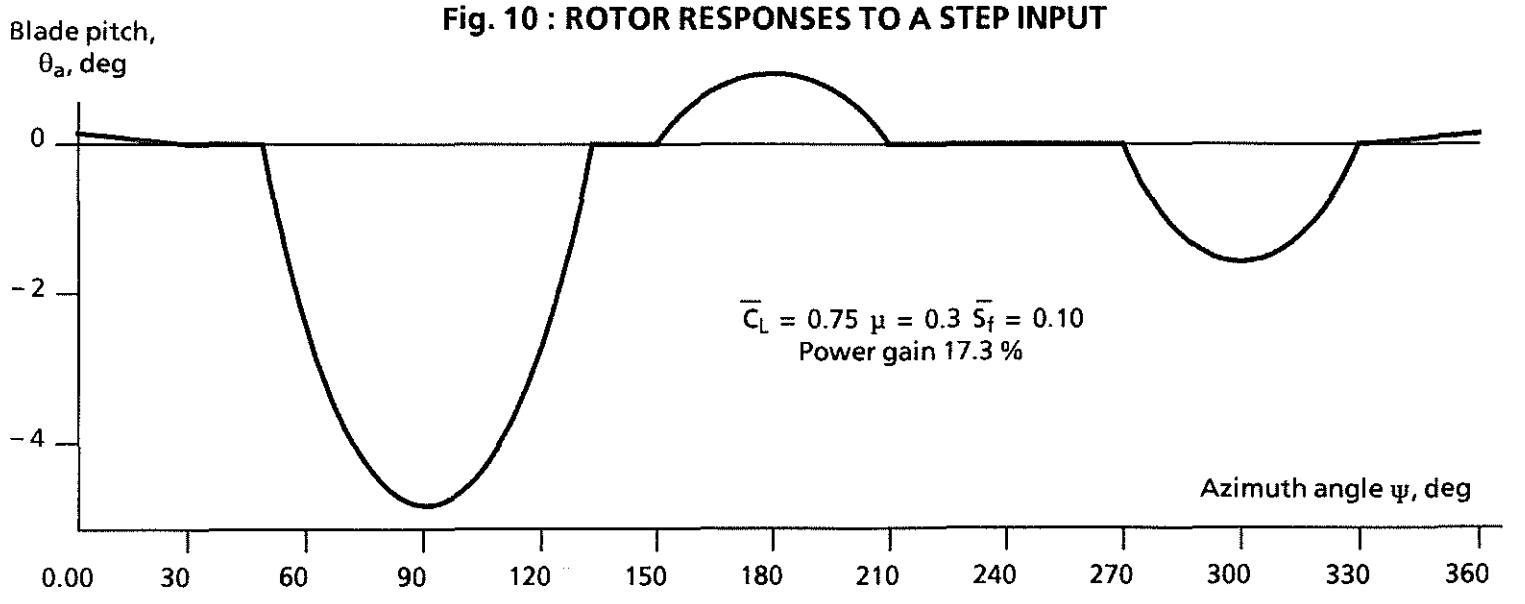


**Fig. 12 : STALL BARRIER FEEDBACK BLADE PITCH**

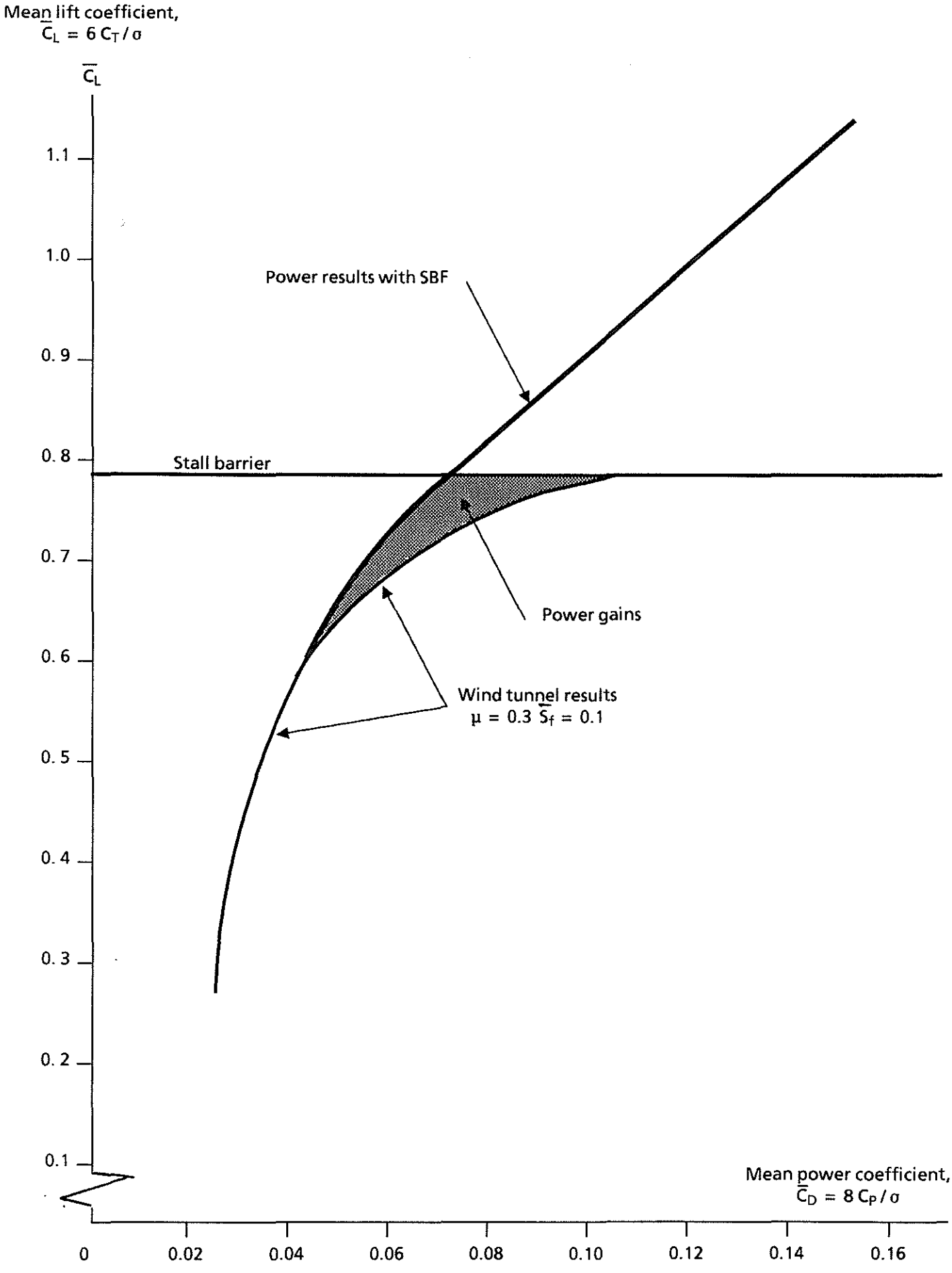


**Fig. 13 : POWER RESULTS OBTAINED WITH ARTIFICIALLY STABILIZED ROTOR : $\mu = 0.3$ , $\bar{S}_f = 0.1$**